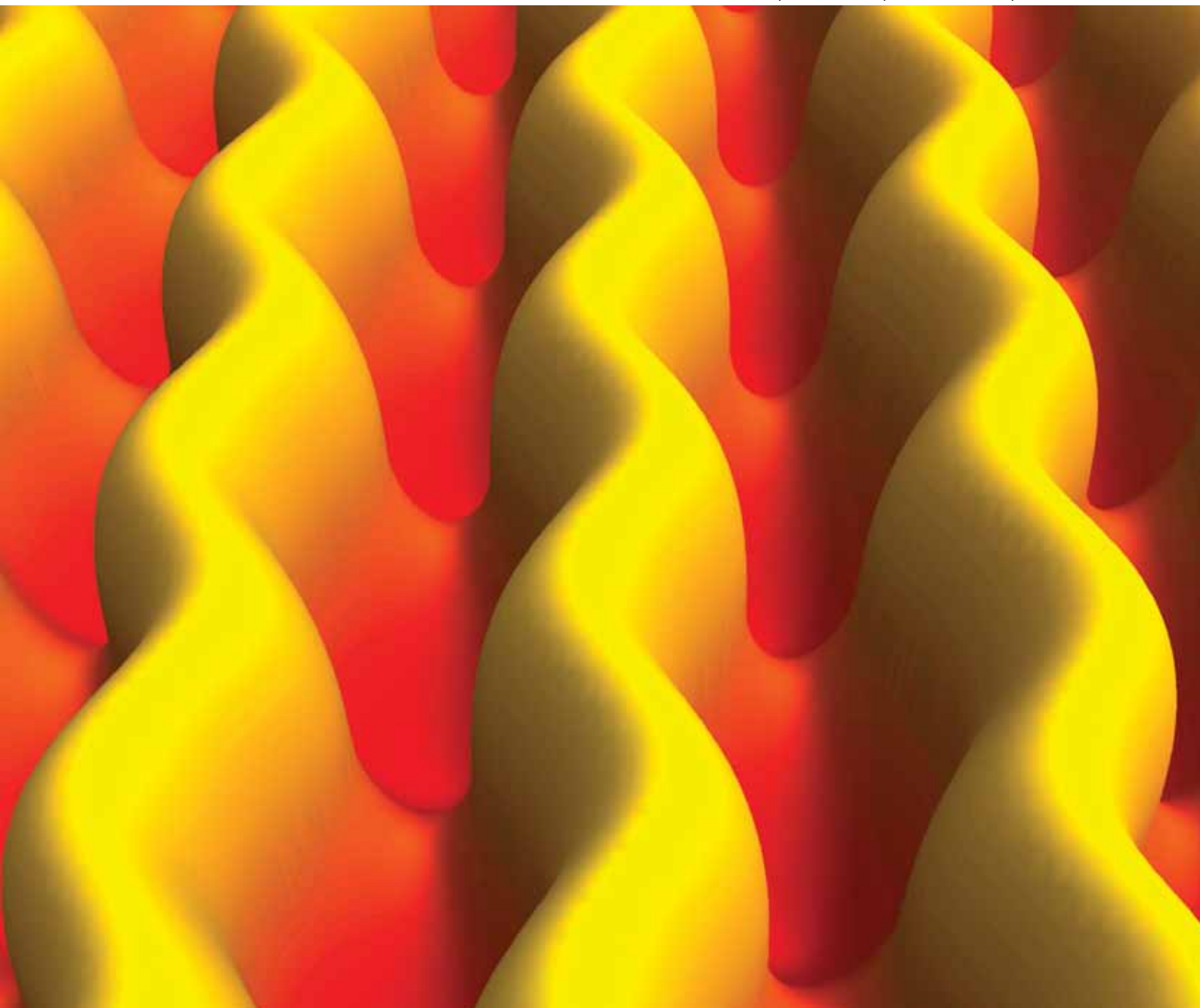


# Soft Matter

www.softmatter.org

Volume 5 | Number 15 | 7 August 2009 | Pages 2817–2972



ISSN 1744-683X

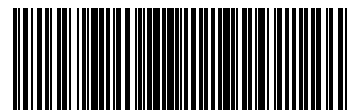
RSC Publishing

**PAPER**

Kyle J. Alvine *et al.*  
Capillary instability in nanoimprinted  
polymer films

**HIGHLIGHT**

E. B. Zhulina and F. A. M. Leermakers  
On the polyelectrolyte brush model of  
neurofilaments



1744-683X(2009)5:15;1-1

# Capillary instability in nanoimprinted polymer films†‡

Kyle J. Alvine,<sup>\*ab</sup> Yifu Ding,<sup>ac</sup> Jack F. Douglas,<sup>\*a</sup> Hyun Wook Ro,<sup>a</sup> Brian C. Okerberg,<sup>a</sup> Alamgir Karim<sup>ad</sup> and Christopher L. Soles<sup>\*a</sup>

Received 23rd January 2009, Accepted 13th March 2009

First published as an Advance Article on the web 21st May 2009

DOI: 10.1039/b901409h

Capillary forces play an active role in defining the equilibrium structure of nanoscale patterns. This effect can be especially pronounced in soft materials such as polymers near or above their glass transition temperature ( $T_g$ ) where material flow is possible. In these situations, the effect of surface tension can produce varied and complex capillary instabilities, even in relatively simple geometries such as parallel-line-space grating patterns. Here we investigate a novel capillary instability that arises upon thermal annealing of nanoimprinted polystyrene line-space gratings with an underlying residual layer. This novel instability is characterized by the development of lateral undulations of the lines, culminating in the localized coalescence of adjacent imprinted lines. An exact analytic model of this undulatory instability is not tractable, but we introduce a simple physical model for this lateral instability based on the driving force to reduce the surface energy, as in the well-known Rayleigh–Plateau instability, which is likewise surface-energy driven. Good agreement is obtained between this simplified model and our observations. Our insights into the nature of this instability have implications for controlling the thermal stability of nanoscale patterns fabricated by nanoimprint lithography or other lithography techniques.

## Introduction

It is well known that capillary (surface tension) forces are of great importance at the nanoscale, specifically in the range of tens to hundreds of nanometres where gravitational forces are negligible and van der Waals forces are still relatively weak. Unfortunately, these surface forces can be quite destructive in the fabrication of nanostructures, and this phenomenon has been reported in association with lithographic processes in particular. Specifically, it is difficult to fabricate high-aspect-ratio features with traditional photolithography due to capillary-force-induced collapse during the rinse step.<sup>1,2</sup> On the other hand, capillary forces can sometimes be beneficial in the lithography process. Upon annealing nanoscale polymer patterns, surface tension can act to reduce line-edge roughness and smooth out pattern defects,<sup>3–6</sup> although this process can also distort essential features, and, under extreme conditions, can cause them to decay completely.<sup>7–12</sup> For this reason and others, there has recently been a great deal of interest in factors that control the thermal stability of nanoscale lithographic patterns and nanostructures.<sup>7–12</sup>

The fact that surfaces with nanoscale topography are unstable to capillary forces can be understood from a simple consideration of the surface energy of these structures. The surface with the lowest surface energy is a planar surface. Thus, a surface with topography is unstable to capillary (or surface tension) forces that tend to smooth the surface. While the simple smoothing of rough edges and height decay noted above are the capillary instabilities that have been observed and studied extensively in the past, we have found that there are *additional* capillary instabilities that can arise in systems with imprinted surface patterns. We focus here on one such instability marked by lateral undulations (see Figs. 1a and b) that occurs upon annealing a simple polymer parallel-line grating (created *via* nanoimprint lithography), where notably there is a residual polymer layer connecting the imprinted lines. A relatively simple model is introduced to explain the origin of this novel undulatory instability.

## Experimental

Nanoscale polymer line-space grating patterns (Fig. 1a) were fabricated *via* the thermal embossing method of nanoimprint lithography (NIL) as outlined schematically in Fig. 1(c–e) and discussed in depth elsewhere.<sup>7–9</sup> Polystyrene (PS) films of molar mass 19.3 kg mol<sup>-1</sup>, 97 kg mol<sup>-1</sup> and 1500 kg mol<sup>-1</sup> with narrow polydispersity index (near 1) were spun onto clean silicon wafers from toluene solutions. Nanopatterns were then formed by NIL with hard line-space grating molds above the  $T_g$  of the PS and at elevated pressure, followed by demolding at  $T < T_g$ . AFM and SEM confirmed the high quality transfer of one-dimensional periodic line-space grating patterns approximately 360 nm in amplitude with pitch or period,  $\Lambda = 424 (\pm 4)$  nm and  $\Lambda = 800 (\pm 3)$  nm into the polymer film, both with nearly 1 : 1 line-to-space ratio. During the imprinting process an approximately

<sup>a</sup>Polymers Division, National Institute of Standards and Technology, Gaithersburg, MD 20899, USA. E-mail: kyle.alvine@pnl.gov; jack.douglas@nist.gov; csoles@nist.gov

<sup>b</sup>Energy and Environment Directorate, Pacific Northwest National Laboratory, Richland, WA 99352, USA

<sup>c</sup>Department of Mechanical Engineering, University of Colorado at Boulder, Boulder, CO 80309-0427, USA

<sup>d</sup>Department of Polymer Engineering, University of Akron, OH 44325, USA

† Work of the US government – Not subject to copyright in the US.

‡ Certain equipment, instruments or materials are identified in this paper in order to adequately specify the experimental details. Such identification does not imply recommendation by the National Institute of Standards and Technology, nor does it imply the materials are necessarily the best available for the purpose.

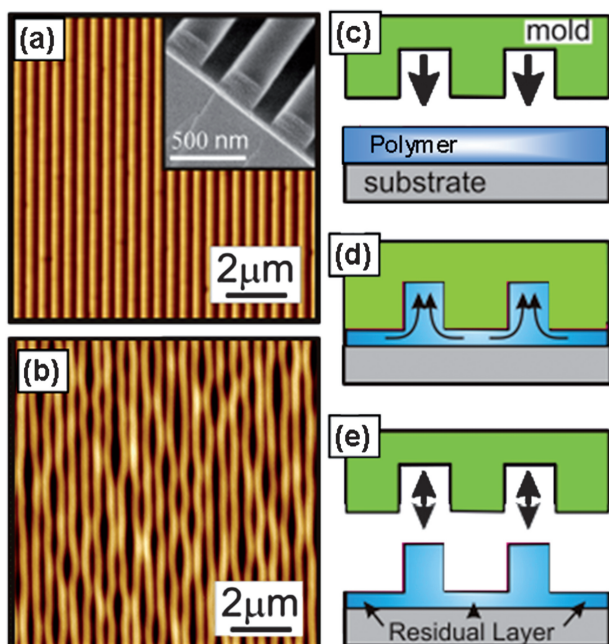


**Fig. 1** (a) AFM image of a typical imprinted polymer line-space grating pattern prior to annealing, and (inset) SEM image showing the cross-section of a typical imprinted pattern prior to annealing. (b) AFM image of a line-space grating (after thermal annealing) demonstrating nearly out-of-phase lateral undulations of the initially parallel polymer lines. (c–e) Schematic illustration of the imprinting process: (c) A nano-patterned mold is brought into contact with the polymer film, and (d) pressed into the film at  $T > T_g$  and elevated pressure, forcing the polymer to flow into the mold. (e) The mold is removed at  $T < T_g$ , leaving the negative pattern with a residual layer of polymer beneath the pattern.

90 nm thick residual layer of polymer is created at the bottom of the pattern (see Fig. 1e) that is left in place for these studies. These patterns offer a simple geometry with which to study the complex interplay of capillary forces.

### A. Simple pattern-height decay ('slumping')

To characterize the nanopattern thermal decay, AFM topography was recorded *ex situ* as a function of annealing time at the polystyrene glass transition temperature,  $T_g = 102\text{ }^\circ\text{C}$ ,  $104\text{ }^\circ\text{C}$ , and  $108\text{ }^\circ\text{C}$  for the respective molar mass PS patterns ( $19\text{ kg mol}^{-1}$ ,  $97\text{ kg mol}^{-1}$ , and  $1500\text{ kg mol}^{-1}$ ). Note that the dimensions (namely height and width) of our features are large enough ( $>50\text{ nm}$ ) that noticeable shifts in  $T_g$  are not a concern.<sup>13</sup> Initially, all patterns exhibited a rounding of the sharp rectangular edges of the pattern, along with decay of the pattern amplitude as observed and discussed in our prior studies of this instability phenomenon in imprinted polymer films.<sup>7–9</sup> The capillary instability governing this rounding and decay can be described in terms of a Laplace pressure,  $P$  acting on the surface topography,  $f(x,y)$ . The Laplace pressure<sup>14</sup> is given by the product of the surface tension  $\gamma$  and the local curvature,  $\kappa \approx f''(x,y)$ . For topography described by a one-dimensional sine function,  $f(x) = (H/2)\sin(2\pi x/\Lambda)$ , the Laplace pressure at the valleys and peaks will have magnitude  $P \approx 2\pi^2\gamma H/\Lambda^2$ , where  $H$  is the line height or twice the pattern amplitude. For simple Newtonian fluids,  $H$  is

predicted<sup>11</sup> to follow a simple exponential decay with time constant  $\tau \approx \eta_{\text{eff}}\Lambda/\pi\gamma$  governed by the effective viscosity  $\eta_{\text{eff}}$ , the pitch, and the surface tension. This rate for pattern-height decay reflects a balance between viscous friction associated with fluid flow and the Laplace pressure. To apply this to our initial rectangular patterns we simply express the topography in terms of a sine series,  $f(x) = \sum A_n \sin(2\pi x/\Lambda_n)$ . Clearly the higher frequency terms in this expansion should damp more rapidly, eventually leaving only the fundamental frequency term (given by the period of the grating). This rationalizes our observations of the rounding of the corners and height decay of the patterned lines, a phenomenon that we refer to as 'slumping'. As mentioned before, this mode of surface-tension-driven pattern decay has been extensively investigated previously.<sup>7–9</sup>

### B. Undulatory capillary instability

By focusing our studies on high imprint temperatures ( $T_{\text{imprint}} \geq T_g + 40\text{ }^\circ\text{C}$ ) and longer annealing times, or by incorporating a surfactant in our films,<sup>15</sup> which enhances the fluidity of the imprinted film, we observe a new type of instability upon annealing that can be described by quasi-periodic and *out-of-phase* lateral undulations of the imprinted lines, a phenomenon that we refer to collectively as the "zigzag instability". These undulations increase in their lateral amplitude with annealing and eventually lead to the merging of the imprinted lines (see Fig. 1b). We find that the occurrence of this instability depends both on the molar mass of the polymer and the imprint temperature  $T_{\text{imprint}}$ , as described below. These lateral undulations have an average wavelength between  $1.5\text{ }\mu\text{m}$  and  $3\text{ }\mu\text{m}$ , determined from a Fourier analysis of AFM and SEM images of the patterns.

The lateral instability does not develop overtly in all patterns and can occur concurrently with pattern-height decay (slumping). We find that the lateral instability develops most strongly in the  $97\text{ kg mol}^{-1}$  and  $1500\text{ kg mol}^{-1}$  PS patterns that were imprinted at *high* temperatures, *i.e.*  $T_{\text{imprint}} = T_g + 80\text{ }^\circ\text{C}$ . The instability is not observed for imprinted patterns of low-molar-mass PS ( $19\text{ kg mol}^{-1}$ ) or for higher-molar-mass PS imprinted patterns formed at lower imprint temperatures,  $T_{\text{imprint}}$  up to  $T_g + 40\text{ }^\circ\text{C}$ . In patterns where the zigzag instability is observed, it is only observed after many hours of annealing (at the respective  $T_g$  for the particular polystyrene). However, the onset time for the growth of this instability, as with the pattern-height decay, is strongly dependent on annealing temperature. Increasing the temperature by a few tens of degrees causes the instability to occur in a matter of minutes. This is evidently caused by the rapid decrease in polymer viscosity with increasing temperature. An exhaustive study of the onset time and development of this zigzag instability as a function of molecular weight and imprint time will be presented in a subsequent publication.

We hypothesize that the dependence on molar mass and imprint temperature is due to a *competition* in the kinetics between the two instabilities: the zigzag mode and the height-decay mode. Our reasoning is based on our previous studies<sup>7–9</sup> where it was demonstrated that the stability of these patterns to height decay is a function of molar mass and imprint temperature. Specifically, the decay time is proportional to the viscosity, which increases rapidly with molar mass, while imprinting at

temperatures near  $T_g$  can result in large amounts of residual stress that will cause rapid pattern decay. Imprinting at high temperatures mitigates these residual stresses. In particular, the patterns most stable to height decay were those that were of relatively high molar mass and imprinted at high imprint temperatures, precisely those patterns which exhibit the onset of the zigzag instability mode. It is also noted that this instability only develops in the 424 nm pitch patterns and not the 800 nm pitch patterns. This singular observation will be discussed in more detail below. Also, we have since observed this zigzag mode in other identical 424 nm patterns fabricated in other polymers, including poly(vinyl acetate), and a commercial fluoropolymer, CYTOP (poly[1,1,2,4,4,5,5,6,7,7-decafluoro-3-oxa-1,6-heptadiene]), indicating that it is not particular to polystyrene. In addition, it was found that the onset of this zigzag mode was greatly accelerated by the addition of a fluorosurfactant, which will be the subject of a future publication.<sup>15</sup> It then appears that this zigzag mode is a *general phenomenon* in imprinted films, governed by viscosity, surface energy and geometry, as expected for a capillary instability.

### Capillary instability model

We next develop a simple physical model to describe the observed zigzag mode as a capillary instability, in a way analogous to the classical Rayleigh–Plateau thread break-up instability where the undulations are likewise driven by a reduction of surface energy of the polymer material. Clearly, such a model must involve mathematical simplification in order to render it analytically tractable; nonetheless, this model is shown below to provide valuable insight into this complex instability. Motivation for our model also comes from the experimental observations of Lee and co-workers<sup>16</sup> where micrometre-scale PS lines ruptured *via* a classical Rayleigh–Plateau instability upon annealing. In these experiments, isolated PS lines were fabricated *without* a residual layer by capillary force lithography.<sup>17</sup> Since the lack of a residual layer implies no interaction between lines, independent break-up of each line occurs. A residual layer allows the lines to *interact* with their neighbors and also to undulate laterally without the energetic cost of moving a contact line with the substrate. When two neighboring lines undulate out-of-phase with each other, there are points where the lines approach and locally coalesce, reducing the total surface area. As in the classical Rayleigh–Plateau instability, the reduction in surface area is the driving factor for the instability. These zigzag undulations also bear remarkable resemblance to the collective out-of-phase break-up of a two-dimensional array of polymer threads in a surrounding immiscible polymer matrix that was observed experimentally by Elemans and co-workers,<sup>18,19</sup> and treated theoretically by Douglas and co-workers<sup>20</sup> and Van de Ven and co-workers.<sup>21</sup> In both experiments and simulations, neighboring threads exhibited out-of-phase zigzag undulations (attributed to a Rayleigh–Plateau capillary instability) followed by adjacent threads collapsing and coalescing. Our system is more complex, due to the three-dimensional nature of the lines and channels, and the competing effect of height decay, yet we see enough similarity to strongly motivate modeling our undulations in terms of a collective Rayleigh–Plateau instability.

### A. Zigzag mode

Nanopatterned surfaces are modeled in piecewise-continuous fashion by separating the pattern into lines (concave down regions) and channels (concave up regions) as shown in Fig. 2a. Cross-sections of both lines and channels are defined by half-ellipses with respective height  $h$ , and width  $w$ , which gives a good approximation to the experiment after the initial stages of annealing have rounded the sharp corners of the pattern, as described earlier. Zigzag undulations are imposed by a perturbation of the line center, defined by amplitude  $A$  and wavelength  $\lambda$  (Fig. 2b). In the ideal case, every line zigzags out-of-phase with its neighbors, requiring the channel width and depth to fluctuate accordingly with the same wavelength in a ‘varicose’ or ‘peristaltic’ mode (Fig. 2c) as the lines coalesce. The functional forms of the line  $f_l(x)$  and channel  $f_c(x)$  cross-sections are given by,

$$f_l(x) = h_l(A) \sqrt{1 - \frac{[x - a(y)]^2}{[w_l/2]^2}} \quad (1)$$

$$f_c(x) = -[h_c(A) - a(y)] \sqrt{1 - \frac{[x + A/2]^2}{[w_c/2 - a(y)]^2}} \quad (2)$$

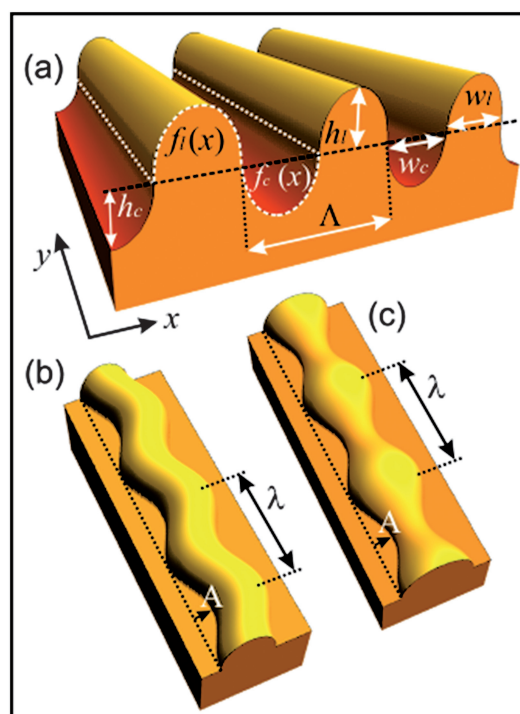


**Fig. 2** (a) Illustration of the piece-wise surface construction used to model the nanopattern. Both lines  $f_l(x)$  (concave down portion, above the horizontal dashed line) and channels  $f_c(x)$  (concave up portion, below the horizontal dashed line) are described by two-dimensional surfaces with half-elliptical cross-sections defined by the height  $h$  and width  $w$  of the line or channel. (b) The zigzag mode is defined by a sinusoidal displacement along the  $y$  direction of the center of the line (or channel). (c) Channels (shown inverted for clarity) are defined by a sinusoidal constriction of the height and width of the channel along the  $y$  direction corresponding to local line coalescence.

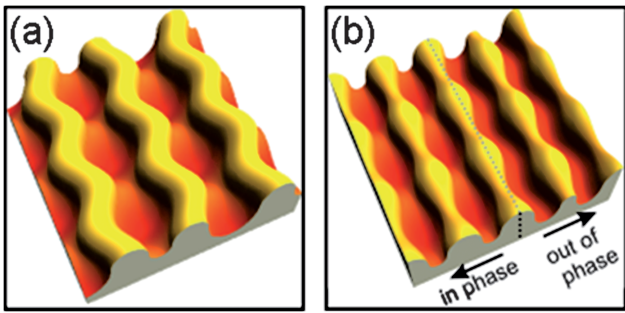


**Fig. 3** (a) Model surface describing the Rayleigh–Plateau instability where the lines zigzag *out-of-phase*. This model shows good qualitative agreement with the AFM data; compare to Fig. 1b. (b) Model surface showing both *in-phase* and *out-of-phase* varicose modes of the lines. These modes are also predicted to be a valid decay mode for this geometry.

$$a(y) = A \sin(2\pi y/\lambda) \quad (3)$$

$$A = w_c + w_l \quad (4)$$

The combined zigzag lines and varicose channels are shown in Fig. 3a. We note that this model surface exhibits very good qualitative agreement with our experimental observations (compare with AFM data Fig. 1b).

Now we demonstrate that the surface undulations described in this model reduce the surface area of the system, consistent with the phenomenon being a capillary instability, and we use our model to provide an estimate of a *lower bound* for the dominant lateral wavelength. Experimental observations require that the average pitch ( $A$ ) and average line and channel widths, ( $w_l$ ,  $w_c$ ) be conserved. We make the further assumption that the volume of polymer material within the lines (and space within the channels) is conserved. Strictly speaking, this is only approximately true since the system is also undergoing simultaneous height decay; however, this decay is happening slowly enough (at the annealing times when the zigzag instability is observed) for this to be a good approximation. Volume conservation is assumed to be local: changes in line volume  $V_l$  (or channel volume,  $V_c$ ) due to the perturbations are compensated for by corresponding changes only in line height  $h_l(A)$  (or channel height  $h_c(A)$ ), yielding:

$$V_l = \frac{\pi}{4} h_l(A) w_l L \approx \frac{\pi \lambda}{4} h_l(A) w_l \left[ 1 + \frac{A^2 \pi^2}{\lambda^2} \right] \quad (5)$$

$$V_c = -\frac{\pi \lambda}{4} [A^2 + h_c(A) w_c] \quad (6)$$

$$h_l(A) \approx h_l \left[ 1 + \frac{A^2 \pi^2}{\lambda^2} \right]^{-1} \quad (7)$$

$$h_c(A) = h_c - \frac{A^2}{w_c} \quad (8)$$

where  $L$  is the arc-length traveled by the center of the line. The surface area  $S$  becomes

$$S_l \approx \frac{\pi L}{2} \left[ h_l(A) + \frac{w_l}{2} \right] \approx \frac{\pi \lambda}{2} \left[ h_l + \frac{w_l}{2} \left[ 1 + \frac{A^2 \pi^2}{\lambda^2} \right] \right] \quad (9)$$

$$S_c \approx \frac{\pi L}{2} \left[ h_c(A) + \frac{w_c}{2} \right] \approx \frac{\pi \lambda}{2} \left[ h_c - \frac{A^2}{w_c} + \frac{w_c}{2} \right] \left[ 1 + \frac{A^2 \pi^2}{\lambda^2} \right] \quad (10)$$

$$S_T = S_l + S_c \approx \frac{\pi \lambda}{2} \left( \left[ 1 + \frac{A^2 \pi^2}{\lambda^2} \right] \left[ h_c - \frac{A^2}{w_c} + \frac{A}{2} \right] + h_l \right) \quad (11)$$

The approximations hold when the aspect ratio ( $h/w$ ) for channels and lines is near 0.5. Eqn (11) implies that the collective perturbations reduce the total surface area when  $\lambda$  satisfies the condition:

$$\lambda \geq \pi \sqrt{\frac{(2h_c + A)w_c}{2}} \quad (12)$$

For the 424 nm pitch sample, this expression yields a *lower bound* for  $\lambda$  of approximately 860 nm for  $h_c = 100$  nm and  $w_c = 240$  nm. The observed wavelength ranges between 1.5  $\mu\text{m}$  and 3.5  $\mu\text{m}$ , a factor of 2–3 larger than the cut-off from our analysis.

The difference between the observed lateral wavelength and the predicted lower cut-off may be due to several factors. First, the dynamics of mass transport have not been included in this model. In fact, the simple surface energy arguments of the classical Rayleigh–Plateau model for a simple cylinder also predict a smaller value than observed. Sophisticated analysis that includes the dynamics were necessary to improve upon the classical prediction.<sup>22</sup> We hope that our simplified model can provide both interest and a starting point for more sophisticated dynamics calculations that are beyond the scope of this paper. Additional effects that may play a role are nucleation effects (one section locks in an out-of-phase zigzag which propagates through the system)<sup>20</sup> or viscoelastic effects, and finally there is the complication of the concurrent height decay. However, the slower kinetics (as compared with the height-decay mode) of the zigzag mode may be rationalized, in part, by the out-of-phase nature of the undulations as this phenomenon may require nucleation (of an out-of-phase region) followed by propagation.

In contrast to the 424 nm pitch patterns, zigzag undulations were absent in the pure PS 800 nm patterns studied. The general lack of zigzag (out-of-phase) pattern undulation with increasing line separation is consistent with the observations in the case of 2D thread arrays.<sup>18,19,21</sup> The channel width is approximately twice as large in the 800 nm patterns as in the 424 nm patterns, implying reduced interaction between lines for oscillatory modes. The absence of the zigzag mode here is likely due to both weaker capillary interactions between lines (for a given height) and an increased mass-flow requirement due to the larger separation between lines.

## B. Varicose modes

We also point out that similar calculations to the ones shown above demonstrate that inversion of surface (shown in Fig. 3a) also leads to a reduction of surface area (see Fig. 3b, RHS), as does a similar mode where both the lines and channels undergo a varicose type of undulation (see Fig. 3b, LHS). Alternatively this can be described as *in-phase* varicose undulations of the lines, whereas in the inverted case the varicose undulations are out-of-phase. A thick residual layer, as in our experiment, would

prevent such varicose undulations in the channels from rupturing the film, as in the experiments of Lee *et al.*<sup>16</sup> without a residual layer. Larger undulations are prohibited by their energetic cost in increasing surface area, though it is probable that this mode could prompt de-wetting in thin enough films. We have since observed a mixture of these varicose-type modes in the case of 800 nm patterns, but only thus far in the presence of a fluorosurfactant, and these results will be discussed further in a future publication<sup>15</sup> as they are beyond the scope of the discussion here.

It is useful to briefly visit the question of mode dominance in these systems. In the case of an isolated thread (no residual layer) the instability modes are fairly restricted. For example, in the case of an isolated non-wetting thread on a surface, slumping is limited to the rounding of the surface due to the line tension. Additionally, Sekimoto and co-workers<sup>23</sup> have shown that the isolated thread is only unstable to varicose and not to zigzag undulations. Thus, the varicose mode is the dominant mode for an isolated thread. This is in line with the observations of Lee *et al.*<sup>16</sup> As noted previously for our system, the residual layer allows the interactions between neighboring lines, and leads to the emergence of collective zigzag modes. Hagedorn *et al.*<sup>20</sup> have shown through lattice Boltzmann simulations that hydrodynamic interactions between 2D threads in an array, through the medium in which the threads are embedded, can make zigzag-like modes, similar to ones we observe, prevalent.

We point out, however, that the energetic model we have set forth here does not yield information about which mode (varicose or zigzag) is dominant. Obtaining this information requires a more sophisticated model that incorporates fluid flow in the residual layer region between the imprinted features, taking into account fluid–substrate interactions and mode coupling. Unfortunately such a model would require substantial numerical calculations (similar to the calculations in 3D of Hagedorn *et al.*) and is beyond the scope of this paper. Nonetheless, our simple geometrical model leads us to expect that the zigzag mode should be kinematically favored over the out-of-phase varicose mode due to the relatively large amount of lateral fluid flow near the substrate required by the latter instability mode.

## Discussion

We have demonstrated a novel type of capillary instability in imprinted polymer films that has broad potential significance in nanotechnology applications. This new instability is marked by nearly out-of-phase lateral undulations and local merger (or collapse) of the lines due to local oscillations. We model these novel zigzag undulations in a manner analogous to the Rayleigh–Plateau thread break-up, where the reduction of the surface energy of the system drives the evolution of the surface morphology. Interactions *via* capillary forces between neighboring lines are made possible through the residual layer of polymer. This relatively simple model incorporates sufficient detail about our complex imprinted pattern geometry and the physical driving forces for instability to provide good qualitative agreement with our observations. We find a good quantitative description of the lateral instability and the prediction of a lower cut-off of the wavelength of the zigzag undulations without the need for laborious numerical simulations. We

note that the collective *out-of-phase* nature of the zigzag instability may indicate slower dynamics as compared with the previously reported height-decay mode. Indeed, we do see that the decay in these systems involves a competition between simple height decay and the zigzag lateral instability where the zigzag mode is only observed when the height decay is sufficiently slow. We also find that the zigzag mode is apparently mitigated in larger spaced patterns, probably due to a reduced interaction between imprinted line features through the fluid underlayer (residual layer). In addition, we have predicted another possible mode where the polymer lines develop a varicose undulation in height and width, with either *in-phase* or *out-of-phase* behavior.

While the patterns used in this study were produced by nanoimprint lithography, it is likely that the results given here should also be applicable to numerous soft matter nanoscale imprinted or lithographically-etched patterns. In many applications involving such structures, the onset of this type of lateral zigzag instability is highly undesirable. Due to time–temperature superposition properties of polymers, the development of instabilities that might take days or longer at one temperature may take seconds at a higher temperature. It is evidently important to understand the physics behind these lateral instabilities to effectively control the stability of this kind of imprinted structure, since such instabilities may distort or completely destroy a device. These types of lateral instabilities may be useful, however, in making complex patterned surfaces for applications where the resulting patterns are desired.

## Acknowledgements

K. J. A. and B. C. O. gratefully acknowledge support from the NIST National Research Council postdoctoral fellowship program. Partial support provided to K. J. A. by Pacific Northwest National Laboratory under DOE contract No. DE-AC05-76RL01830 is gratefully acknowledged. Use of the NIST Combinatorial Methods Center equipment and the Materials Science and Engineering Laboratory Electron Microscopy Facility is gratefully acknowledged. We also thank C. M. Stafford for insightful discussions.

## References

- 1 H. B. Cao, P. F. Nealey and W. D. Domke, Comparison of resist collapse properties for deep ultraviolet and 193 nm resist platforms, *J. Vac. Sci. Technol., B*, 2000, **18**, 3303–3307.
- 2 M. P. Stoykovich, H. B. Cao, K. Yoshimoto, L. E. Ocola and P. F. Nealey, Deformation of nanoscopic polymer structures in response to well-defined capillary forces, *Adv. Mater.*, 2003, **15**, 1180–1184.
- 3 S. Y. Chou and Q. F. Xia, Improved nanofabrication through guided transient liquefaction, *Nat. Nanotechnol.*, 2008, **3**, 295–300.
- 4 C. Y. Chao and L. J. Guo, Reduction of surface scattering loss in polymer microrings using thermal-reflow technique, *IEEE Photonics Technol. Lett.*, 2004, **16**, 1498–1500.
- 5 C. Y. Chao and L. J. Guo, Thermal-flow technique for reducing surface roughness and controlling gap size in polymer microring resonators, *Appl. Phys. Lett.*, 2004, **84**, 2479–2481.
- 6 Z. N. Yu, L. Chen, W. Wu, H. X. Ge and S. Y. Chou, Fabrication of nanoscale gratings with reduced line edge roughness using nanoimprint lithography, *J. Vac. Sci. Technol., B*, 2003, **21**, 2089–2092.

- 
- 7 Y. F. Ding, H. W. Ro, J. F. Douglas, R. L. Jones, D. R. Hine, A. Karim and C. L. Soles, Polymer viscoelasticity and residual stress effects on nanoimprint lithography, *Adv. Mater.*, 2007, **19**, 1377–1382.
  - 8 R. L. Jones, T. J. Hu, C. L. Soles, E. K. Lin, R. M. Reano and D. M. Casa, Real-time shape evolution of nanoimprinted polymer structures during thermal annealing, *Nano Lett.*, 2006, **6**, 1723–1728.
  - 9 H. W. Ro, Y. F. Ding, H. J. Lee, D. R. Hines, R. L. Jones, E. K. Lin, A. Karim, W. L. Wu and C. L. Soles, Evidence for internal stresses induced by nanoimprint lithography, *J. Vac. Sci. Technol., B*, 2006, **24**, 2973–2978.
  - 10 E. Buck, K. Petersen, M. Hund, G. Krausch and D. Johannsmann, *Macromolecules*, 2004, **37**, 8647–8652.
  - 11 M. Hamdorf and D. Johannsmann, Decay kinetics of nanoscale corrugation gratings on polymer surface: Evidence for polymer flow below the glass temperature, *J. Chem. Phys.*, 2000, **112**, 4262–4270.
  - 12 K. Petersen and D. Johannsmann, Measurements on the surface glass transition of PMMA from the decay of imprinted surface corrugation gratings: the influence of molecular weight, *J. Non-Cryst. Solids*, 2002, **307**, 532–537.
  - 13 C. M. Stafford, B. D. Vogt, C. Harrison, D. Julthongpipit and R. Huang, Elastic moduli of ultrathin amorphous polymer films, *Macromolecules*, 2006, **39**, 5095–5099.
  - 14 A. W. Adamson and A. P. Gast, *Physical Chemistry of Surfaces*, Wiley, New York, 3rd edn, 1997.
  - 15 K. J. Alvine, Y. F. Ding, H. W. Ro, J. F. Douglas, A. Karim and C. L. Soles, unpublished work.
  - 16 J. Park, K. Y. Suh, S. Seo and H. H. Lee, Anisotropic rupture of polymer strips driven by Rayleigh instability, *J. Chem. Phys.*, 2006, **124**, 5.
  - 17 K. Y. Suh, Y. S. Kim and H. H. Lee, Capillary force lithography, *Adv. Mater.*, 2001, **13**, 1386–1389.
  - 18 P. H. M. Elemans, J. M. vanWunnik and R. A. vanDam, Development of morphology in blends of immiscible polymers, *AIChE J.*, 1997, **43**, 1649–1651.
  - 19 Y. M. M. Knops, J. J. M. Slot, P. H. M. Elemans and M. J. H. Bulters, Simultaneous breakup of multiple viscous threads surrounded by viscous liquid, *AIChE J.*, 2001, **47**, 1740–1745.
  - 20 J. G. Hagedorn, N. S. Martys and J. F. Douglas, Breakup of a fluid thread in a confined geometry: droplet-plug transition, perturbation sensitivity, and kinetic stabilization with confinement, *Phys. Rev. E*, 2004, **69**, 18.
  - 21 A. Y. Gunawan, J. Molenaar and A. A. F. Van de Ven, Break-up of a set of liquid threads under influence of surface tension, *J. Eng. Math.*, 2004, **50**, 25–49.
  - 22 S. Tomotika, On the Stability of a Cylindrical Thread of a Viscous Liquid surrounded by another Viscous Fluid, *Proc. R. Soc. London, Ser. A*, 1935, **150**, 322–337.
  - 23 K. Sekimoto, R. Oguma and K. Kawasaki, Morphological stability analysis of partial wetting, *Ann. Phys.*, 1987, **176**, 359–392.